Original Article

CT features of lung scar cancer

Feng Gao[1*], Xiaojun Ge[1*], Ming Li[1,2], Xiangpeng Zheng[2], Li Xiao[3], Guozhen Zhang[2], Yanqing Hua[1]

[1]Department of Radiology, [2]Diagnostic and Treatment Center of Small Lung Nodules, [3]Department of Pathology, Huadong Hospital Affiliated to Fudan University, Shanghai 200040, China

*These authors contributed equally to this work.

Correspondence to: Ming Li. Diagnostic and Treatment Center of Small Lung Nodules/Department of Radiology, Huadong Hospital Affiliated to Fudan University, Shanghai 200040, China. Email: minli77@163.com.

Objective: To explore the CT features of lung scar cancer (LSC).

Methods: CT images of 41 LSCs and 66 non-LSCs were retrospectively compared in terms of location, size, shape, border, speculation, lobulation, pleural indentation, surrounding ground-glass opacification (sGGO), vessel convergence, vacuolation, calcification and satellite opacification.

Results: Thirty-eight LSCs were histopathologically identified as adenocarcinoma. The LSCs and non-LSCs were located 8.73±8.65 and 12.55±10.67 mm from the pleura, respectively. The mean lesion sizes (3-D ratios) in the initial LSC, pre-surgical LSC and non-LSC images were 24.28±6.29 (0.33±0.65), 32.23±8.14 (0.60±0.18) and 23.24±3.73 (0.35±0.61) mm, respectively. The initial and pre-surgical LSC images showed significant differences in speculation and sGGO ($P<0.05$). Significant differences were also noted in vacuolation, vessel convergence and sGGO between the pre-surgical LSC and the non-LSC images ($P<0.05$) and in vacuolation between the initial LSC and the non-LSC images ($P<0.05$).

Conclusions: Despite similar CT features of LSCs and non-LSCs, the early detection and diagnosis of LSCs is possible by studying scar-tissue changes such as enlargement and sGGO associated with well-defined lesion borders in follow-up CT images.

Keywords: Lung neoplasms; cicatrix; tomography; X-ray computed; adenocarcinoma

Submitted Oct 11, 2014. Accepted for publication Jan 21, 2015.
doi: 10.3978/j.issn.2072-1439.2015.02.07
View this article at: http://dx.doi.org/10.3978/j.issn.2072-1439.2015.02.07

Introduction

Lung scar cancer (LSC) was first reported by Friedrich in 1939. LSC originates from scar tissues in the lung and periphery locations (1). LSC has no specific symptoms, and the tumours always overlap existing scar tissues. LSC can be easily misdiagnosed as an old lesion, delaying treatment (2). Furthermore, it has poor prognosis because of metastasis from relatively small lesions (1,3,4). With the growing popularity of regular lung CT screening, more and more suspected LSCs have been diagnosed by radiologists. The early detection and diagnosis of LSC is critical for better treatment outcomes. In this retrospective study, we aim to explore the CT features of LSC.

Materials and methods

Patients

This study included CT images of 41 patients (28 men and 13 women; age range, 44-90 years; mean age, 68.39± 12.52 years) with histopathologically confirmed LSC obtained between February 2006 and April 2014. No patient had previous primary tumours. All underwent two or more chest CT scans over a mean interval of 23.47± 17.53 months (range, 3 months to 5 years 11 months), including scans within 2 weeks before surgery or biopsy. The clinical presentations include history of tuberculosis and local scars after treatment (14 cases), cough and sputum (nine cases), chest pain (six cases), chest distress and

Table 1 Locations of the LSCs and non-LSCs

Location	LSCs (n=41)	Non-LSCs (n=66)
Right upper lobe	21	14
Right middle lobe	1	4
Right lower lobe	5	12
Superior segment	4	3
Basal segments	1	9
Left upper lobe	12	29
Left lower lobe	2	7
Superior segment	1	1
Basal segments	1	6

LSC, lung scar cancer.

shortness of breath (three cases) and no symptoms (nine cases).

CT images of 66 patients (45 men and 21 women; age range, 27-84 years; mean age, 62.52±12.79 years) with non-LSCs were also examined for comparison. Sixty cases were confirmed follow-up CT scans, and six cases were confirmed by histopathology. Among these confirmed by histopathology, there are two cases of tuberculous granuloma, one case of inflammatory granuloma and three cases of organized pneumonia. All patients received two or more chest CT examinations. The minimum follow-up period was 3 years, and the maximum was 12 years and 2 months (mean, 62.83±24.21 months).

Image analysis

Chest CT (range from the apex to the base of the lung, including the chest wall and axillary fossa) scans were performed with a 64-detector CT system (GE Light Speed VCT or GE Discovery CT750 HD, GE Healthcare, Milwaukee, WI, USA) by using the following scan parameters: 1.25-mm section width, 1.25-mm reconstruction interval, pitch of 0.984, 120 kV and 250 mA (64-detector CT system) or 16-detector CT system (Sensation 16, SIMENS, Germany) by using the following scan parameters: 1mm section width, 1mm reconstruction interval, pitch of 1, 120 kV and 150 mA. Standard high-resolution methods were used for image reconstruction.

Two chest radiologists (Ming Li and Xiangpeng Zheng, with 15 and 18 years of experience in chest CT, respectively), who were blinded to the histopathological results, evaluated the CT scans in consensus. The assessed features included location (measured as the distance between the lesion and the pleura), size (average of the maximum values along three dimensions in MPR images), 3-D ratio (minimum values along three dimensions/maximum values along three dimensions), calcification, vacuolation, border, speculation, lobulation, pleural indentation, surrounding ground-glass opacification (sGGO), satellite opacification and vessel convergence (window width/window level: mediastinal window, 350/50; lung window, 1,500/–500).

Statistical analysis

Statistical analyses were performed with commercially available software (SPSS 16.0 for Windows, SPSS, Inc., Chicago, IL, USA). Pearson chi-square test and independent *t*-test were used to compare categorical and numerical data, respectively. The level of statistical significance was set as $P<0.05$.

Results

All the LSC sand non-LSCs were solitary lesions (*Table 1*). The LSCs include done case of large cell carcinoma, two cases of squamous cell carcinoma and 38 cases of adenocarcinoma.

The average distances of the LSCs and non-LSCs to the pleura were 8.73±8.65 and 12.55±10.67 mm, respectively; 8 and 14 of the respective lesions were connected to the pleura (distance of 0 mm). The difference in distance to the pleura between the LSCs and the non-LSCs was not significant (t=0.147, P=0.56).

Significant differences in lesion size (t=–4.950, P=0.000) and 3-D ratio (t=–9.318, P=0.000) were noted between the initial and the pre-surgical LSC images (*Table 2*, *Figure 1*). The pre-surgical LSC and non-LSC images also showed significant differences in lesion size (t=–6.649, P=0.000) and 3-D ratio (t=–8.807, P=0.000). Lesion size (t=0.953, P=0.345) and 3-D ratio (t=–1.776, P=0.079) were not significantly different between the initial LSC and the non-LSC images.

The initial and pre-surgical LSC images showed significant differences in speculation and sGGO (*Figures 2* and *3*) but not the other features. Moreover, significant differences in vacuolation, vessel convergence and sGGO were noted between the presurgical LSC and the non-LSC images (*Figure 4*). The initial LSC and non-LSC images showed a significant difference in vacuolation only (*Table 3*). Eight LSCs showed sGGO with a well-defined border in the

Table 2 Comparison of the CT findings

Feature	Initial LSC images (n=41) (%)	Presurgical LSC images (n=41) (%)	Non-LSC images (n=66) (%)
Size (mm)	24.28±6.29	32.23±8.14	23.24±3.73
3-D ratio	0.33±0.65	0.60±0.18	0.35±0.61
Irregular/polygonal shape	32 (78.05)	29 (70.73)	47 (71.21)
Long spiculation border	17 (41.46)	19 (46.34)	39 (59.09)
Speculation	6 (14.63)	15 (36.59)	13 (24.53)
Lobulation	18 (43.90)	24 (58.54)	35 (53.03)
Pleural indentation	33 (80.79)	35 (85.37)	49 (74.24)
sGGO	11 (26.83)	26 (63.41)	8 (12.12)
Vessel convergence	10 (24.39)	18 (43.90)	7 (10.61)
Vacuolation	14 (34.15)	15 (36.59)	6 (9.09)
Calcification	10 (24.39)	10 (24.39)	28 (42.42)
Satellite opacification	11 (26.83)	11 (26.83)	23 (34.85)

The values represent mean ± SD or number of lesions (%). LSC, lung scar cancer; sGGO, surrounding ground-glass opacification.

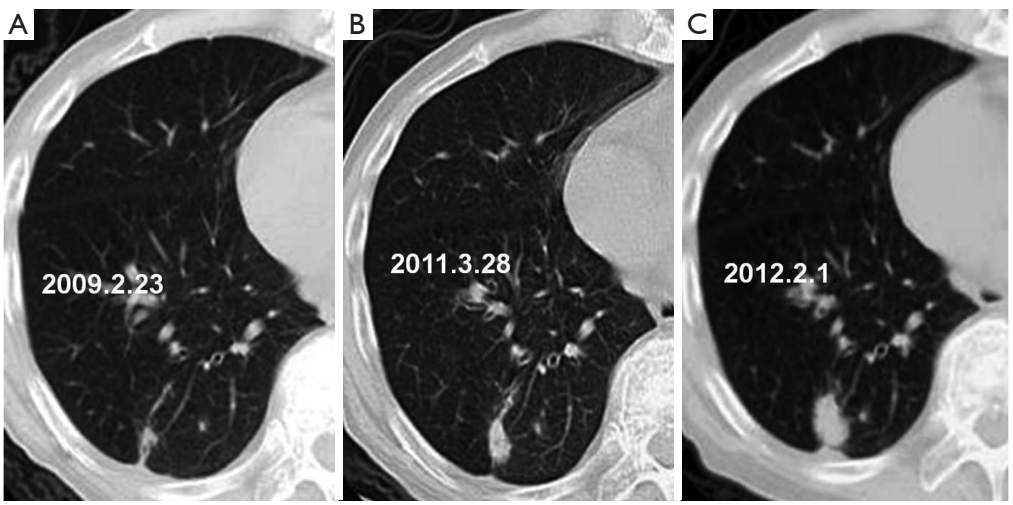

Figure 1 CT images of the lower lobe of the right lung. A spiculation and gradual enlargement of the peripheral lesion are visible over the 3-year follow-up (A-C). The lesion was confirmed as adenocarcinoma by histopathology.

follow-up images (*Figures 5* and *6*) and thirty three LSCs were enlarged (*Figure 1*).

Discussion

LSC was first reported by Friedrich in 1939. Most lesions are smaller than 3 cm and localised to the periphery of the upper lobe of the lungs. LSC shows male predominance and is mainly adenocarcinoma or peripheral lung cancer (1,5-7). In the case of adenocarcinoma, fibrosis or scarring (hyalinosis) may be present at the centre of the tumour (5). Intensive fibrotic degeneration and carbon powder decomposition is visible on the cut surface. Adenocarcinomatous cells are arranged in small nests or a single layer. Sometimes, a few malignant cells are localised to the interlobar pleura or subpleural area. LSCs tend to show early lymph-node metastasis and small-vessel invasion (1), resulting in a lower 5-year survival rate (5%) than the general 5-year survival rate of adenocarcinomas (22%) and adenosquamouscarcinomas (28%). Therefore, LSC should be suspected when a new lesion emerges in a lung scar or a focal scar shows enlargement in follow-up

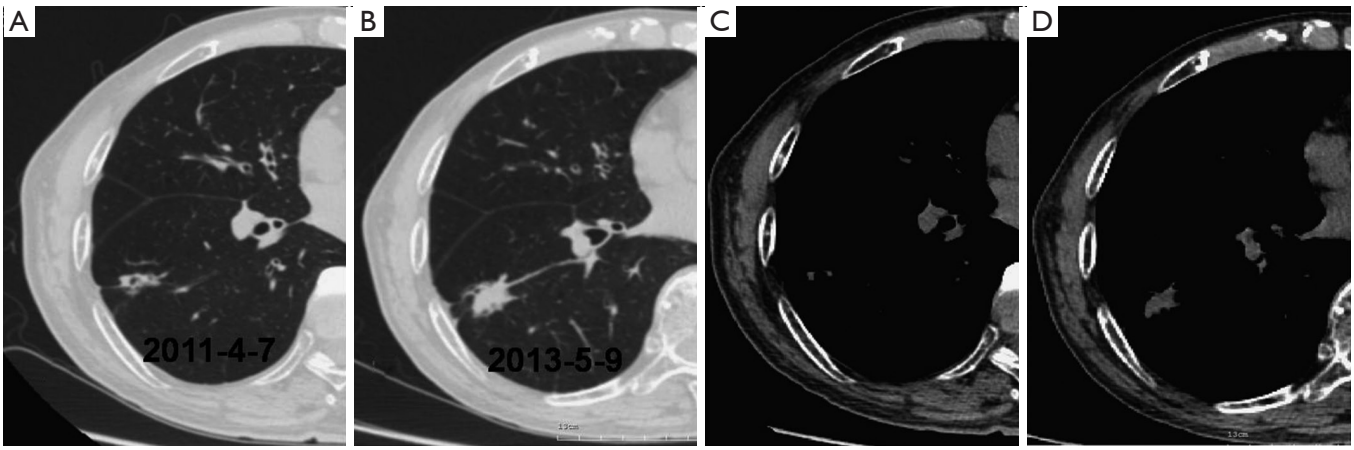

Figure 2 CT images of the lower lobe of the right lung obtained in the (A and B) lung window and (C and D) mediastinal window. The nodule in the initial scans (A and C) appears enlarged in the follow-up scans (B and D).

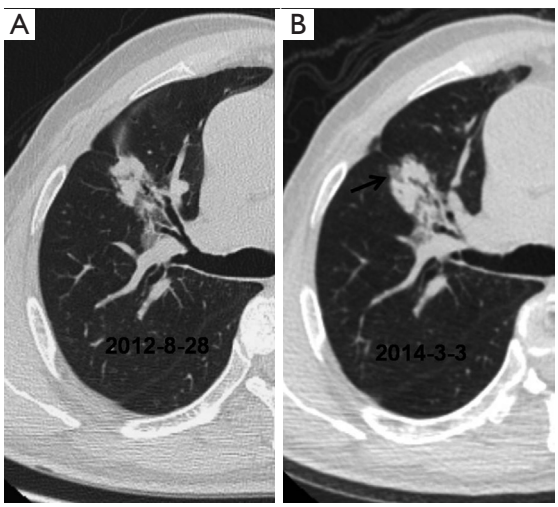

Figure 3 CT images of the upper lobe of the right lung. The nodule in the initial scan (A) appears larger in the follow-up image (B) and shows sGGO (arrow). sGGO, surrounding ground-glass opacification.

CT images.

Lung scars may occur secondary to tuberculosis, bronchiectasis, pulmonary abscess, organized pneumonia, trauma or infarction, with tuberculosis being the most common cause (5,8). The pathogenesis of LSC is not clear. It could result from chronic inflammation of a lung scar (9-11). Repeated injury and repair process over a long period stimulates bronchial and alveolar epithelium, ultimately causing atypical hyperplasia or canceration of focal lesions (12-15). Fibrosis can disturb or block lymphatic drainage and result in pooling of cancer cells in the scar (12), causing more extensive vascular and lymphatic seeding in scar cancer than in regular adenocarcinoma or squamous cell carcinoma (16).

LSCs tend to occur at the predilection sites of lung tuberculosis (1,6). The mean diameter of LSCs secondary to tuberculosis has been reported as 5.3 cm (2), which is greater than the average diameter (3.5 cm) in our study. In this study, 33 of 39 lesions (84.62%) showing enlargement in follow-up CT images were histopathologically identified as LSCs. Eight lesions did not grow in size but subsequently showed some sGGOs. The eight non-LSCs that showed sGGOs had a fuzzy border. Although not an absolute evidence for LSC diagnosis, lesion enlargement or emergence of sGGOs with clear lesion borders is highly suggestive of LSC.

The distance between the LSCs and the pleura is shorter than 1cm, supporting previous reports (6,17). However, this feature has no obvious value for differential diagnosis between LSCs and non-LSCs.

Calcification and satellite opacification are common CT features of pulmonary tuberculosis and generally regarded as benign signs. In the present study, these features were not significantly different between the LSC and the non-LSC images. This result could be explained by the fact that the LSCs are mostly originated from old tuberculous lesions (2,18,19). Therefore, regular follow-up of scar-tissue lesions is advisable because of the possibility of malignant transformation.

Some studies showed that benign lesions often have an irregular or polygonal shape and long spiculation

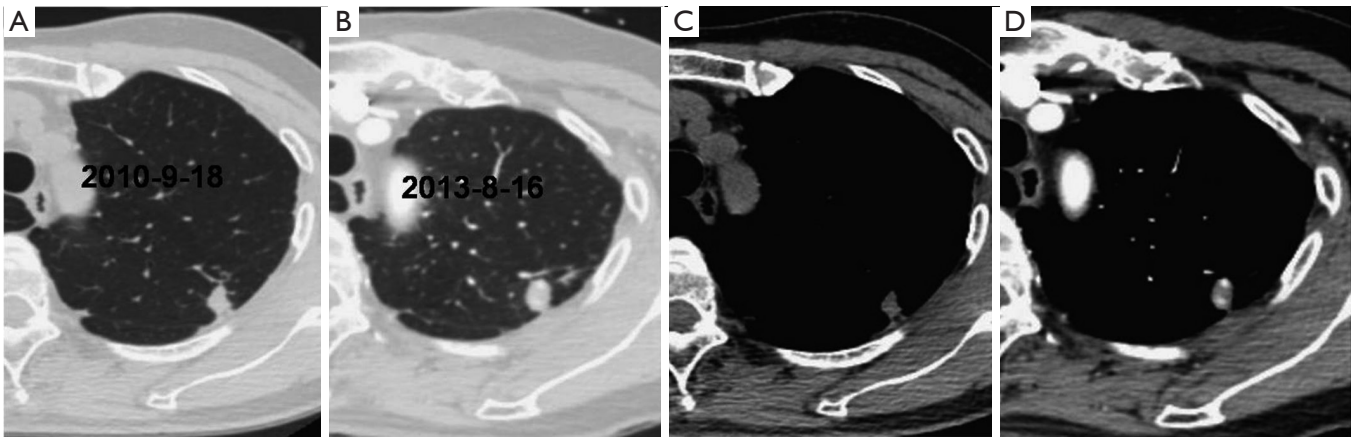

Figure 4 CT images of the upper lobe of the left lung obtained in the (A and B) lung window and (C and D) mediastinal window. The nodule in the initial scans (A and C) has enlarged and shows calcification in the follow-up scans (B and D).

Table 3 Statistical results

Feature	Initial *vs*. presurgical LSC images		Presurgical LSC *vs*. non-LSC images		Initial LSC *vs*. non-LSC images	
	χ^2	P	χ^2	P	χ^2	P
Irregular/polygonal shape	0.576	0.448	0.003	0.958	0.612	0.434
Long spiculation border	0.198	0.656	1.656	0.198	3.150	0.076
Speculation	5.185	0.023	3.733	0.053	0.444	0.505
Lobulation	1.757	0.185	0.310	0.578	0.843	0.359
Pleural indentation	0.345	0.557	1.854	0.173	0.551	0.458
sGGO	11.081	0.001	30.693	0.000	3.746	0.053
Vessel convergence	3.471	0.062	15.659	0.000	3.596	0.058
Vacuolation	0.054	0.817	12.120	0.000	10.446	0.001
Calcification	0.000	1.000	3.591	0.058	3.591	0.058
Satellite opacification	0.000	1.000	6.750	0.386	0.750	0.386

LSC, lung scar cancer; sGGO, surrounding ground-glass opacification.

border (20,21). We found that both LSCs and non-LSCs manifested an irregular or polygonal shape, long spiculation border and pleural retraction. Therefore, these features have little diagnostic value. Alveolar structure collapse, local organisation or other factors in LSCs may cause focal tissue injury, fibrosis, shrinkage and retraction of adjacent structures, resulting in the irregular shape and long spiculation border of such tumours. Pleural indentation appears when the pleura is retracted by fibrosis. Fibrosis stimulated by cancerous tissues may form a lung scar, which may look similar to LSC in CT images and confuse diagnosis (22). Our findings show that scar-tissue formation preceded canceration in all cases.

Lobulation, speculation and vessel convergence are common in LSCs. Although the initial LSC and non-LSC images did not show significant differences in these features, vessel convergence was significantly different between the pre-surgical LSC and non-LSC images. These findings suggest the importance of regular follow-up of lung scars showing vessel convergence in CT images. We should also suspect LSC in emerging speculations in former lesions.

Connective-tissue hyperplasia is promoted by scar-tissue formation and may produce air cavities. LSCs originate in bronchiolar or alveolar epithelium. Vacuolation occurs when partially aerated lung tissue is not replaced by tumorous tissue. It may also form as a result of overly air-filled alveolar cavities blocked by tumorous invasion. The spread of tumorous cells in surrounding lung tissues can be

Figure 5 CT images of the apex of the right lung. A spiculation is visible in the initial image (A). The lesion gradually enlarges in the follow-up images (B and C) and shows sGGO (arrows). sGGO, surrounding ground-glass opacification.

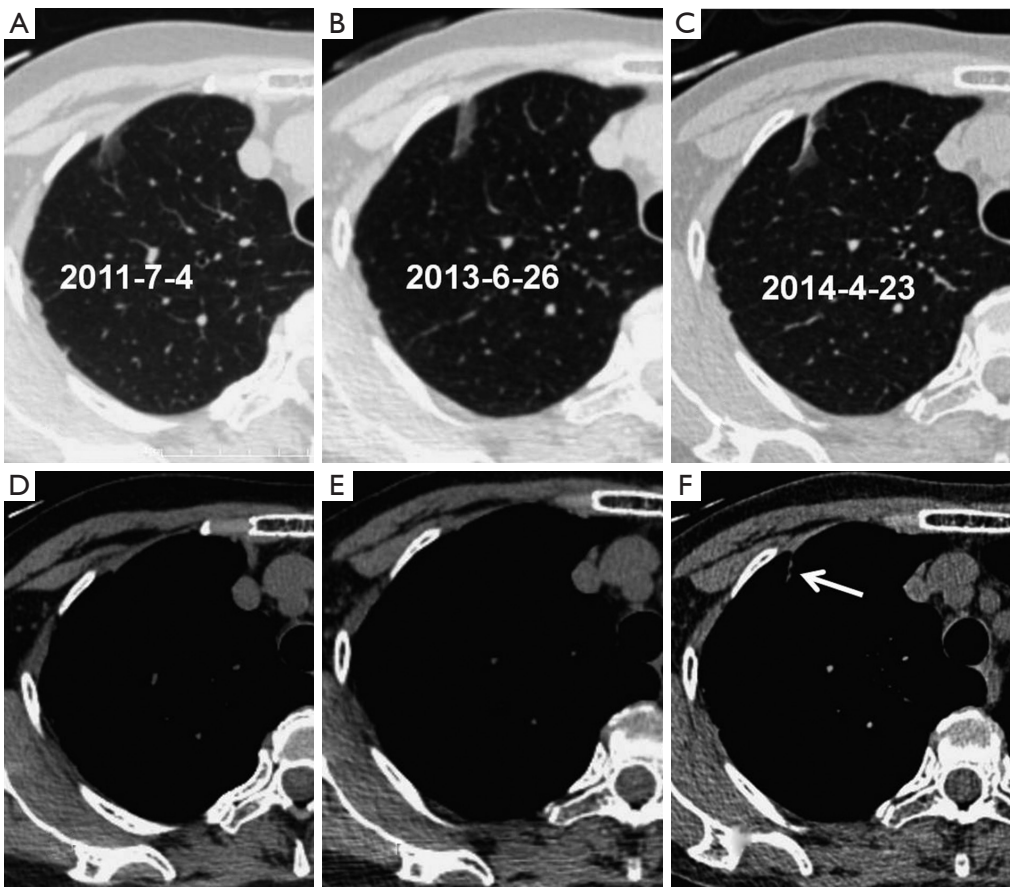

Figure 6 CT images of the apex of the right lung obtained in the (A-C) lung window and (D-F) mediastinal window. The lesion in the initial images (A and D) gradually enlarges over the 3-year follow-up (B,C,E,F) and shows sGGO (arrow). sGGO, surrounding ground-glass opacification.

manifested as GGO in CT images when these cells do not completely occupy the alveolar cavities. GGO can be caused by inflammation, but the borders of inflammatory lesions are obscure whereas those of LSCs are well defined. Recent studies have indicated that vacuolation and sGGO can help to differentiate between benign and malignant lesions (23,24). Since these features are less common in non-LSC images, they can be helpful in LSC diagnosis.

Well-defined ground glass opacities, surrounding previously existing lung scar tissues, can be considered as the manifestation of early stage LSCs. These well-defined ground glass opacities may solidify gradually if no early intervention is taken. Most LSCs are adenocarcinomas, and their emergence and development are similar to those of adenocarcinomas.

We observed overlaps between lung scar tissues and LSC on CT images. Thus, LSC diagnosis is very difficult based on a single CT image. Radiologists may misdiagnose early-stage LSCs as old lesions if sequential CT images are not examined.

The differential diagnosis of LSC includes recurrent pulmonary tuberculosis and pneumonia. LSC should be suspected in patients with a history of pulmonary tuberculosis who present cough, blood phlegm and negative results for acid-fast bacilli. However, some recurrent tuberculous lesions may be confused for LSC if they show enlargement, speculation and lobulation in follow-up CT exams. Furthermore, organised tissue could appear gradually at the site of malabsorption of pneumonia, and are similar to LSC as a result of increased fibrosis caused by chronic inflammation and pleural thickening. It can also grow in size in follow-up CT images. Two cases of organized pneumonia showed subsequent enlargement in our study. We recommend a follow-up schedule of 3-6 months based on the malignant risk if diagnosis is difficult from initial CT images.

In conclusion, periodic CT scans are necessary for early diagnosis of LSC. Scar-tissue changes such as enlargement, speculation and sGGO associated with a well-defined border in follow-up CT images should be considered as indications of LSC.

Acknowledgements

Funding: This work has been financially supported by the National Natural Science Foundation of China (Grant No. 81472794), Shanghai Municipal Commission of Health (20134360), Shanghai Municipal Commission of Science and Technology (24119a0400), Key talents training program of Huadong Hospital (HDGG2014011).
Disclosure: The authors declare no conflict of interest.

References

1. Freant LJ, Joseph WL, Adkins PC. Scar carcinoma of the lung. Fact or fantasy? Ann Thorac Surg 1974;17:531-7.
2. Kim YI, Goo JM, Kim HY, et al. Coexisting bronchogenic carcinoma and pulmonary tuberculosis in the same lobe: radiologic findings and clinical significance. Korean J Radiol 2001;2:138-44.
3. Lee BY, Guerra J, Cagir B, et al. Pulmonary scar carcinoma: report of three cases and review of the literature. Mil Med 1995;160:537-41.
4. Terzakis JA. X-ray microanalysis of peripheral lung carcinomas. Ultrastruct Pathol 1995;19:167-73.
5. Madri JA, Carter D. Scar cancers of the lung: origin and significance. Hum Pathol 1984;15:625-31.
6. Yokoo H, Suckow EE. Peripheral lung cancers arising in scars. Cancer 1961;14:1205-15.
7. Balo J, Juhasz E, Temes J. Pulmonary infarcts and pulmonary carcinoma. Cancer 1956;9:918-22.
8. Bobba RK, Holly JS, Loy T, et al. Scar carcinoma of the lung: a historical perspective. Clin Lung Cancer 2011;12:148-54.
9. Wahl SM. Inflammation and growth factors. J Urol 1997;157:303-5.
10. Uhl EW, Castleman WL, Sorkness RL, et al. Parainfluenza virus-induced persistence of airway inflammation, fibrosis, and dysfunction associated with TGF-beta 1 expression in brown Norway rats. Am J Respir Crit Care Med 1996;154:1834-42.
11. Kovacs EJ. Fibrogenic cytokines: the role of immune mediators in the development of scar tissue. Immunol Today 1991;12:17-23.
12. Ardies CM. Inflammation as cause for scar cancers of the lung. Integr Cancer Ther 2003;2:238-46.
13. Kitagawa M. Autopsy study of lung cancer with special reference to scar cancer. Acta Pathol Jpn 1965;15:199-222.
14. Chaudhuri MR. Primary pulmonary scar carcinomas. Indian J Med Res 1973;61:858-63.
15. Raeburn C, Spencer H. A study of the origin and development of lung cancer. Thorax 1953;8:1-10.
16. Carroll R. The influence of lung scars on primary lung cancer. J Pathol Bacteriol 1962;83:293-7.
17. Auerbach O, Garfinkel L, Parks VR. Scar cancer of the lung: increase over a 21 year period. Cancer 1979;43:636-42.

18. Nuessle WF. Association of bronchogenic carcinoma and active pulmonary tuberculosis; with report of four cases. Dis Chest 1953;23:207-16.
19. Steinitz R. Pulmonary tuberculosis and carcinoma of the lung. A survey from two population-based disease registers. Am Rev Respir Dis 1965;92:758-66.
20. Li F, Sone S, Abe H, et al. Malignant versus benign nodules at CT screening for lung cancer: comparison of thin-section CT findings. Radiology 2004;233:793-8.
21. Kohno N, Ikezoe J, Johkoh T, et al. Focal organizing pneumonia: CT appearance. Radiology 1993;189:119-23.
22. Shimosato Y, Suzuki A, Hashimoto T, et al. Prognostic implications of fibrotic focus (scar) in small peripheral lung cancers. Am J Surg Pathol 1980;4:365-73.
23. Kojima Y, Saito H, Sakuma Y, et al. Correlations of thin-section computed tomographic, histopathological, and clinical findings of adenocarcinoma with a bubblelike appearance. J Comput Assist Tomogr 2010;34:413-7.
24. Nambu A, Araki T, Taguchi Y, et al. Focal area of ground-glass opacity and ground-glass opacity predominance on thin-section CT: discrimination between neoplastic and non-neoplastic lesions. Clin Radiol 2005;60:1006-17.

Cite this article as: Gao F, Ge X, Li M, Zheng X, Xiao L, Zhang G, Hua Y. CT features of lung scar cancer. J Thorac Dis 2015;7(3):273-280. doi: 10.3978/j.issn.2072-1439.2015.02.07